

Electronic Supplementary Information

Ligand triggered antenna effect and dual emissions in Eu(III) MOF and its application in multi-mode sensing of 1,4-dioxane

Madhulekha Gogoi^{1*}, Sanmilan Jyoti Kalita^{1,2}, Jyotirmoy Deb³, Ankur Gogoi⁴ and Lakshi Saikia^{1,2*}

¹Advanced Materials Group, Materials Sciences & Technology Division, CSIR-North East Institute of Science and Technology, Jorhat-785006, Assam, India

²Academy of Scientific and Innovative Research, Ghaziabad 201002, India

³Advanced Computational & Data Sciences Division, CSIR-North East Institute of Science and Technology, Jorhat-785006, Assam, India

⁴Department of Physics, Jagannath Barooah University, Jorhat-785001, Assam, India

Corresponding author's e-mail ID: l.saikia@gmail.com/lsaikia@neist.res.in

Synthesis of g-C₃N₄. 20 gm (0.26 mol) of thiourea was taken in a silica crucible and heated in a furnace at temperature 550 °C for 2 h with lid covered. After cooling to room temperature, 1.6 gm of yellow powder of bulk C₃N₄ was obtained. This was again heated at 550 °C for 2 h with lid open. Finally, 0.38 gm of white powder of g-C₃N₄ was obtained.

For exfoliation, 129 mg of g-C₃N₄ was dispersed in a mixture of 10 mL water and 10 mL isopropyl alcohol in a 150 mL beaker. Then the solution was ultrasonicated with the help of a probe sonicator in an ice bath for 48 h (continuous for 30 min, break for 5 min). After sonication, the solution was allowed to stand for 12 h and the precipitate was discarded by decantation. The supernatant was centrifuged at 10,000 rcf for 6 min. The precipitate obtained such was oven dried at 60 °C for 12 h. The powder obtained weighed ~ 103 mg.

Functionalization of g-C₃N₄ with benzoic acid (BCN). 1.267 gm (7 mmol) of 2-aminoterephthalic acid and 280 mg of NaOH (7 mmol) were added to 80 mL of water and

stirred in an icebath. When temperature reached 5 °C, 526 mg (4 mmol) of NaNO₂ was added to it slowly. Then 6 mL (19.2 mmol, 6.4 M) of 20% HCl solution was added quickly to it followed by 45 min stirring. At the instant of HCl addition, the solution became pale yellow in color and later creamish precipitate was formed. The powder of phenyl carboxylic diazonium salt was obtained by filtration with Whatman 41 (diameter 110 mm) filter paper and oven drying at 60 °C for 12 h.

For functionalizing the carboxylic acid groups on g-C₃N₄ sheets, 300 mg of it was dispersed in 50 mL of 1% (w/v) sodium dodecyl sulphate solution in water by sonication. When temperature reached ~ 7 °C, 300 mg of above prepared phenyl carboxylic diazonium salt was added to it and stirred at 5 °C for 4 h and then at room temperature for another 4 h. The powder of functionalized g-C₃N₄ was obtained by centrifuging the above solution at 10,000 rpm for 6 min and by oven drying the precipitate at 60 °C for 12 h. Yield is 570 mg. It was named as BCN.

Synthesis of composite of BCN with MoS₂ (MSBCN). 50 mg of BCN and 2.6 mg of MoS₂ were mixed and dispersed in 50 mL ethanol by sonication for 2 h. Then, the solution was heated to evaporate ethanol and then dried in oven for 1 h at 60 °C. In this way, 5% (w/w) composite of greyish color was obtained with a yield of ~ 40 mg.

Synthesis of MOF from Eu³⁺ ions and BCN (MZN-1). 73 mg (1 mmol) of EuCl₃.6H₂O and 7.3 mg (10% by wt) of functionalized g-C₃N₄ (BCN) were added to 50 mL N,N-dimethylformamide and mixed by sonication. Then the solution was stirred magnetically for 1 h and then put in an autoclave of 100 mL capacity at 130 °C for 48 h. Creamish precipitate was obtained after centrifugation at 7000 rpm for 10 min and washing with ethanol and acetone. It was oven dried at 60 °C for 12 h. Yield is ~ 47 mg.

Synthesis of MOF from Eu³⁺ ions, terephthalic acid (BDC) and MSBCN (MZN-2). 264 mg (0.7 mmol) of EuCl₃.6H₂O and 20 mg (7% by wt) of MSBCN were dispersed in 20

mL DMF. It was mixed with a solution of terephthalic acid prepared by dissolving 58 mg (0.35 mmol) of BDC in 40 mL DMF. The resulting solution was stirred at room temperature for one h and then put in an autoclave of 100 mL capacity at 130 °C for 48 h. The creamish powder was obtained after centrifugation, washing with ethanol-acetone, oven drying at 60 °C for 12 h. Yield is ~ 200 mg.

CHARACTERIZATION OF THE Eu-MOF:

The Fourier Transform infrared spectroscopy (FT-IR) data were obtained by FTIR Spectrum (SPECTRUM TWO, PerkinElmer, USA) using Attenuated Total Reflectance (ATR) method. The optical characterization of the samples was carried out with SPECORD® 210 PLUS spectrophotometer (Analytik Jena, Germany) for measuring absorption spectra in the range of 200-800 nm at room temperature. Morphological study of the samples were performed using high resolution transmission electron microscope (HRTEM) by JEM-2100 Plus electron microscope (JEOL, USA) and field emission scanning electron microscope (FESEM) by Carl ZEISS microscope (SIGMA, Germany). The elemental compositions and energy dispersive X-ray (EDX) elemental mapping were obtained from energy dispersive X-ray spectroscopy (EDS) attached with FESEM. Compositional study of the samples and valence band maxima calculation were carried out with X-ray photoelectron spectroscopy (XPS) on ESCALAB Xi+ (EXCALAB Xi+, Thermo Fisher Scientific Pvt. Ltd., USA). On the other hand all the fluorescence study and fluorescence lifetime measurement were taken in Horiba Scientific Fluorolog-3 fluorescence spectrophotometer (Horiba, Japan).

Fluorescence sensing study. In order to check the fluorescence based sensing of 1,4-dioxane, a solution of MZN-2 was prepared by dispersing 2.5 mg of it in 2.5 mL water followed by sonication. Then fluorescence spectra was recorded by exciting with 270 nm. The sensing experiment was performed by adding an increasing volume of dioxane solution with stirring

and recording the fluorescence spectra at same excitation wavelength. The response time was calculated to be as fast as 5 s.

Gas phase sensing study. Next, we investigate whether the MOF we have created has the ability to function as a direct electrical sensor for volatile organic compound dioxane. The sensor response was recorded in terms of the electrical current signal change in the gaseous environment at room temperature. For that the powder MOF sample was compressed to a pellet of thickness 1.2 ± 2 mm and diameter of 1.3 cm. The gas chamber system was constructed on a vacuum desiccator of DN 140 mm by modifying the top portion so that the custom-built 2-point probe can be connected. The sample pellet was loaded into this 2-point probe system and the electrical response was real-time recorded with the help of an electrometer (2401, Keithley). The outline of the setup is shown in Fig. 14(a). At first, the electrical signal of the pellet was recorded against increasing voltage input in air. We allowed 30 sec to stabilize the signal before recording. Then sensing gas environment of dioxane was prepared by keeping a petri dish filled with the volatile liquid at the base of the desiccator. And after loading the sample pellet in this environment, air inside the desiccator was evacuated with the help of a vacuum pump. The results were plotted in the form of I-V characteristic curves along with time.

Computational Methodology.

Structural optimization of these systems has been conducted without applying any symmetry constraints using the density functional theory methodology (DFT) as prescribed in the Gaussian 09 computational package.^{S1} Becke's three parameters Lee–Yang–Parr hybrid functional (B3LYP)^{S2} along with def2-SVP basis set for Eu atom and 6-31G(d) basis set for rest of the atoms has been used in the calculation. The characterization of the saddle point's properties is determined through frequency calculations. These structures have indeed attained true local minima on the potential energy surface, as evidenced by the presence of entirely real

frequencies. Solvent phase calculation has been performed using water as a solvent with the help of the integral equation formalism polarizable continuum model (IEFPCM).

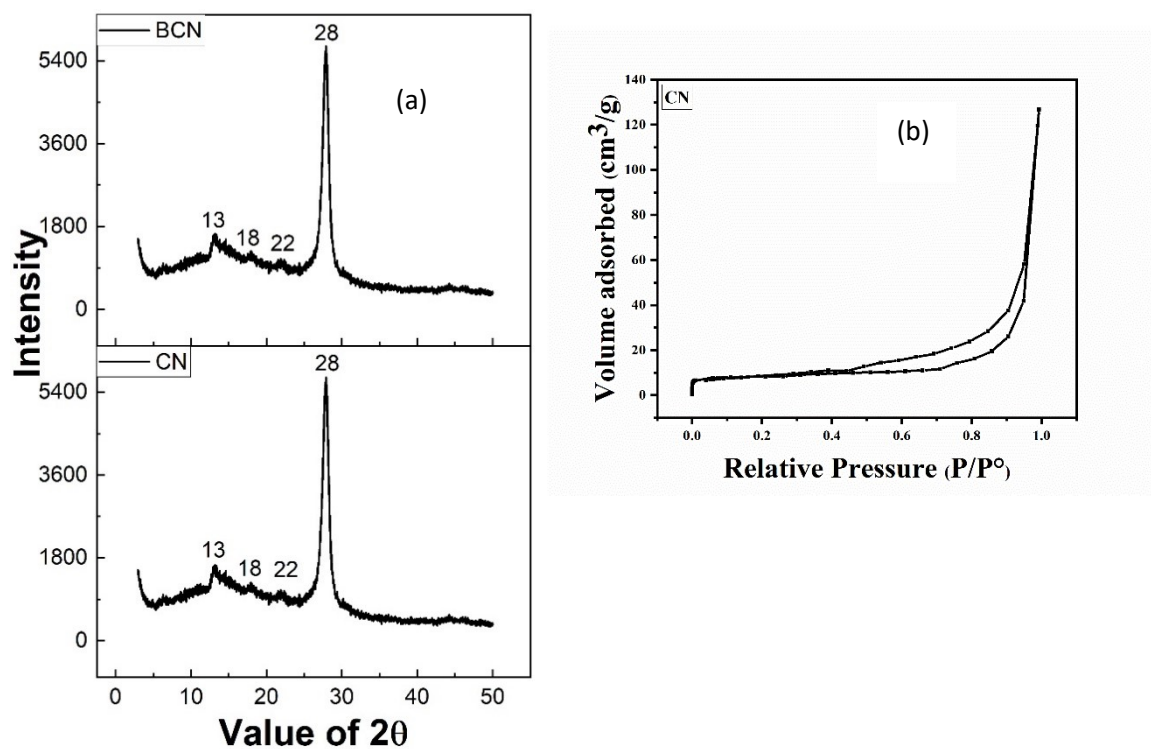


Fig. S1 (a) Comparative XRD pattern of CN and BCN and (b) BET isotherms of CN.

Table S1: BJH data

S. No.	Samples	Surface area (m ² /g)	Pore volume (cm ³ /g)	Pore diameter (Å)
1	CN	32.38	0.19	40.26
2	BCN	25.357	0.13	15.6
3	MSBCN	6.814	0.052	15.618
4	MZN-1	6.456	0.028	33.16

5	MZN-2	15.058	0.056	30.60
6	MZN-2R	133.196	0.226	24.477

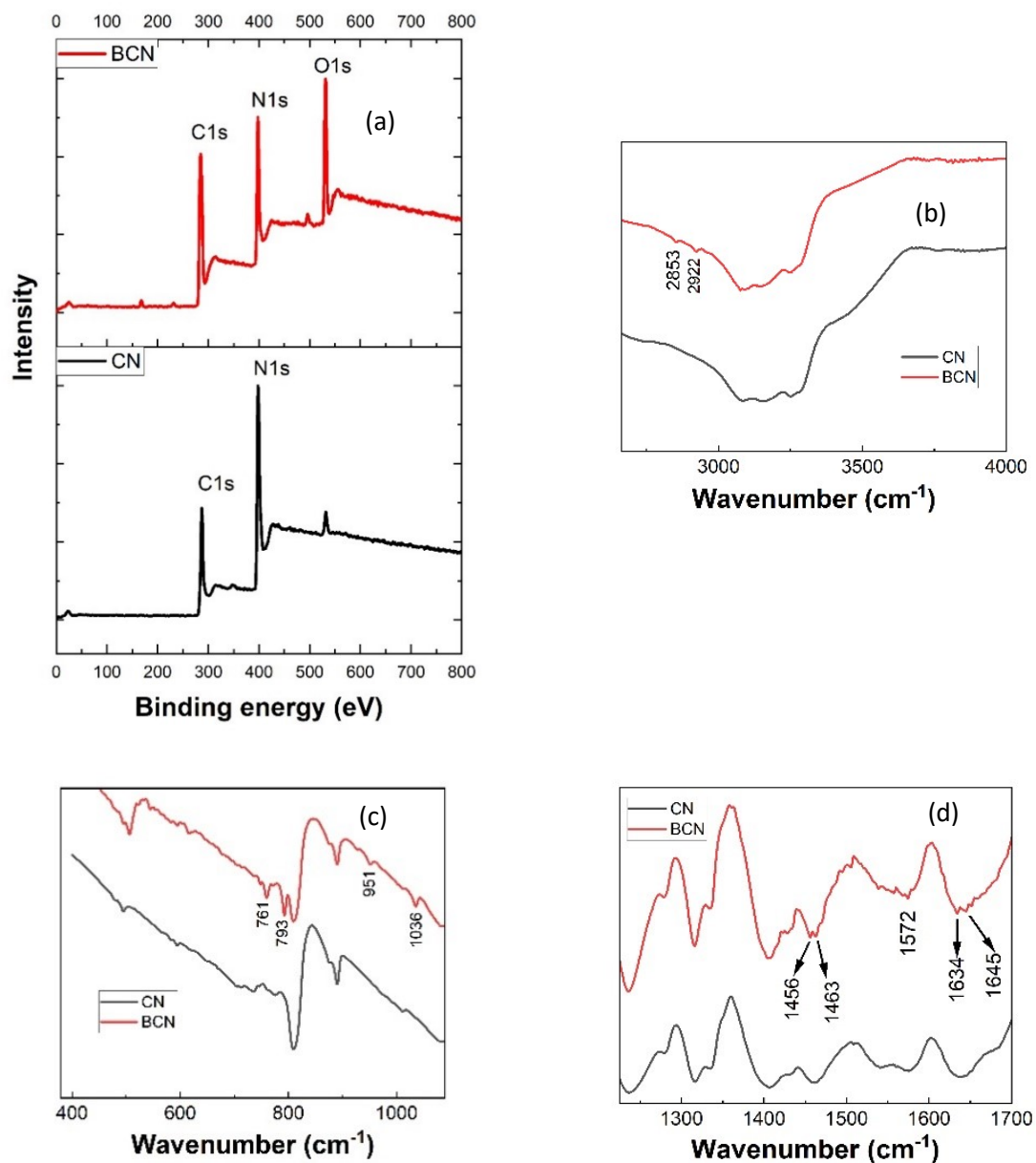


Fig. S2. (a) XPS survey spectra and (b), (c), (d) FTIR spectra of CN and BCN in different ranges.

Interpretation of FTIR spectra of CN and BCN: The FTIR spectra are presented in Fig. S2, ESI, while from the FTIR spectra of BCN in Fig. S2 (b), new peaks are observed at 2853 and 2922 cm^{-1} related to protonated N-H^+ absorption.^{S3} Also, bands appearing in BCN spectra at 793 and 961 cm^{-1} corroborate to O-H translational and liberation vibrations.^{S4} However, as observed from Fig. S2(c) and (d), the broad peaks of CN spectra split into smaller peaks in case of BCN, which are assigned accordingly. Among these, 1572 cm^{-1} is assigned to $\text{C}=\text{C}$ and 1634 cm^{-1} to $\text{C}=\text{O}$ band of benzoic acid.^{S5}

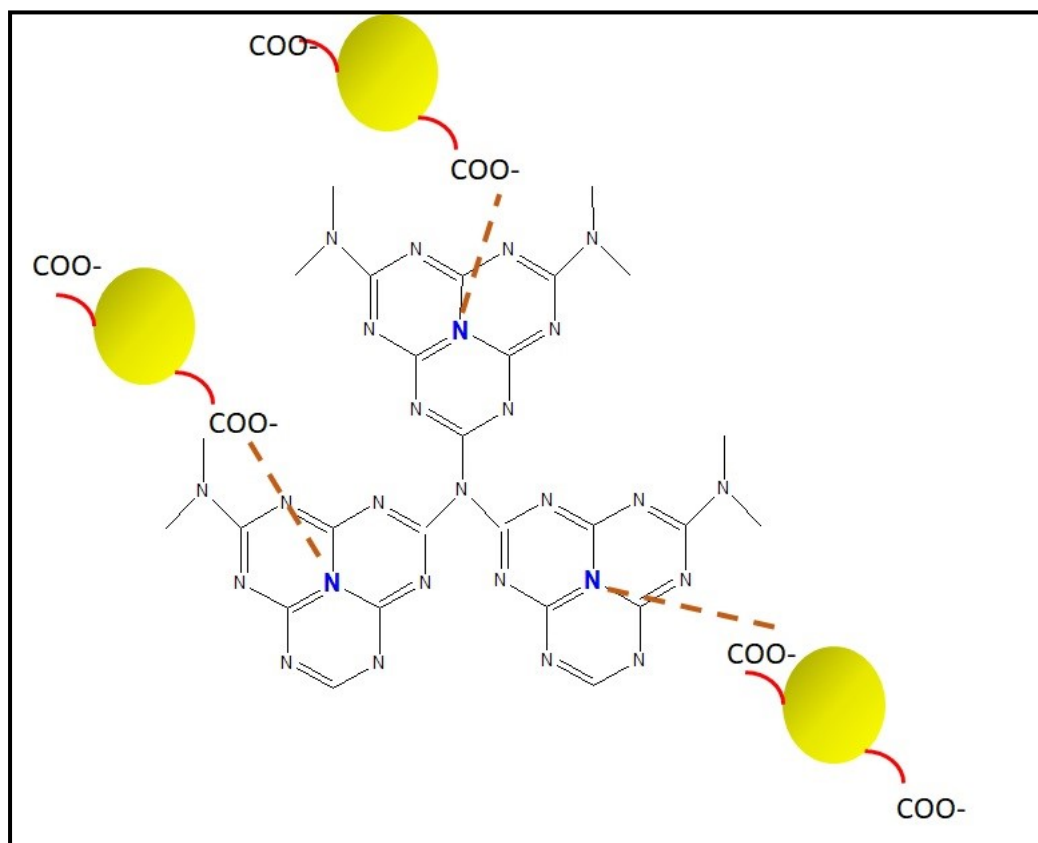


Fig. S3. Plausible schematic diagram of BCN. Where, the yellow block represents benzoic acid which is bonded to $\text{g-C}_3\text{N}_4$ sheets through $\text{NH}\cdots\cdots\text{O}$ kind of hydrogen bonding.

Table S2: XPS Peak details of BCN, MZN-1 and MZN-2

C1s			
Sample name	Peak position	Peak position	Peak position
BCN	284.6 eV (C-C)	287.8 eV (C-N ₃)	
MZN-1	284.6 eV	288.6 eV	289.9 eV
MZN-2	283.7 eV	287.1 eV	
N1s			
BCN	398.4 eV	399.7 eV	403 eV
MZN-1	398.4 eV	400.2 eV	
MZN-2	397.6 eV	399.4 eV	
O1s			
BCN	531.7 eV	533.3 eV	
MZN-1	532.6 eV		
MZN-2	530.7 eV		
Eu3d			
MZN-1	1125.7 eV	1135.3 eV	
MZN-2	1124.7 eV	1134.3 eV	
S2p			
MZN-2	161.4 eV	166.4 eV	

Table S3: Elemental composition of BCN, MZN-1 and MZN-2 from XPS

BCN										
Elements	C1s	N1s	O1s							
Atomic %	49.6	32.1	18.3							
MZN-1										
Elements	C1s	N1s	O1s	Eu3d3	Eu3d5					
Atomic %	51.57	1.82	45.74	0.37	0.5					
MZN-2										
Elements	C1s	N1s	O1s	Eu3d3	Eu3d5	S2p1	S2p	S2p3	Mo3d3	Mo3d
Atomic %	43.45	2.08	41.82	0.23	0.36	6.47	2.19	3.3	0.04	0.05

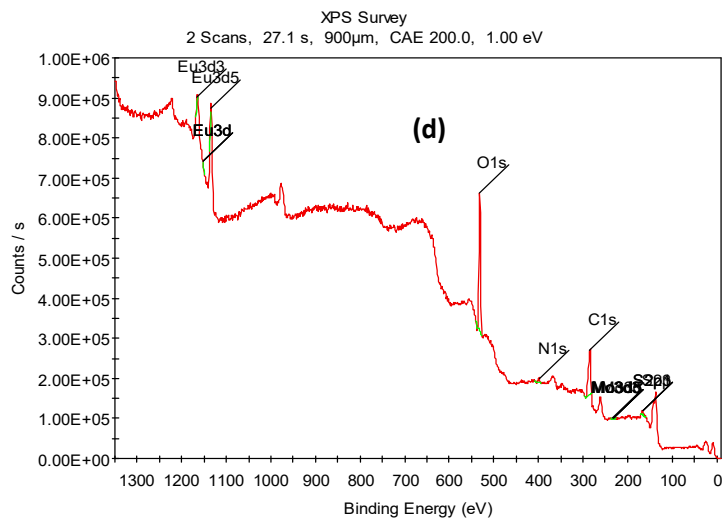
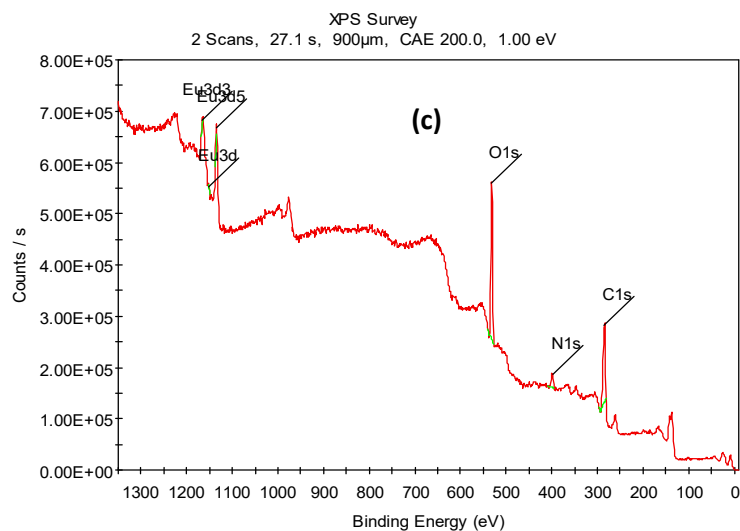
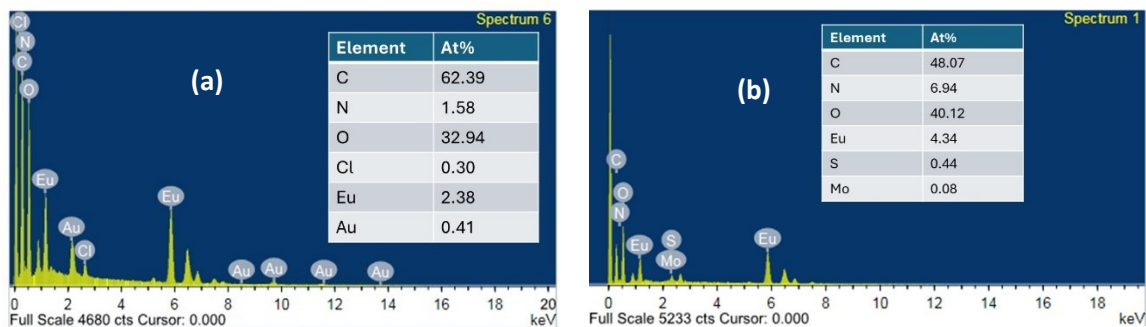


Fig. S4. EDS spectra of (a) MZN-1 and (b) MZN-2. XPS survey spectra of (c) MZN-1 and (d) MZN-2.

Table S4: Atomic percentage of elements from XPS survey spectra

MZN-1		MZN-2	
Element	At%	Element	At%
O1s	38.06	O1s	41.82
N1s	6.38	N1s	2.08
C1s	55.09	C1s	43.45
Eu3d3	0.15	Eu3d3	0.23
Eu3d	0.02	Eu3d5	0.36
Eu3d5	0.3	S2p1	6.47
		S2p	2.19
		S2p3	3.3

Table S5: SAED analysis of MZN-1

	Area	Mean	Min	Max	Angle	Length (1/D)	1/r	r (nm)	d spacing (Å)
1	0.058	60.691	0.016	255	-64.586	3.401	1.7005	0.588	5.88
2	0.1	106.56	3.63E-04	255	-36.307	5.885	2.9425	0.339	3.39
3	0.145	73.536	0	255	113.394	8.514	4.257	0.2349	2.349
4	0.206	91.812	0.012	255	-78.895	12.103	6.0515	0.1652	1.652

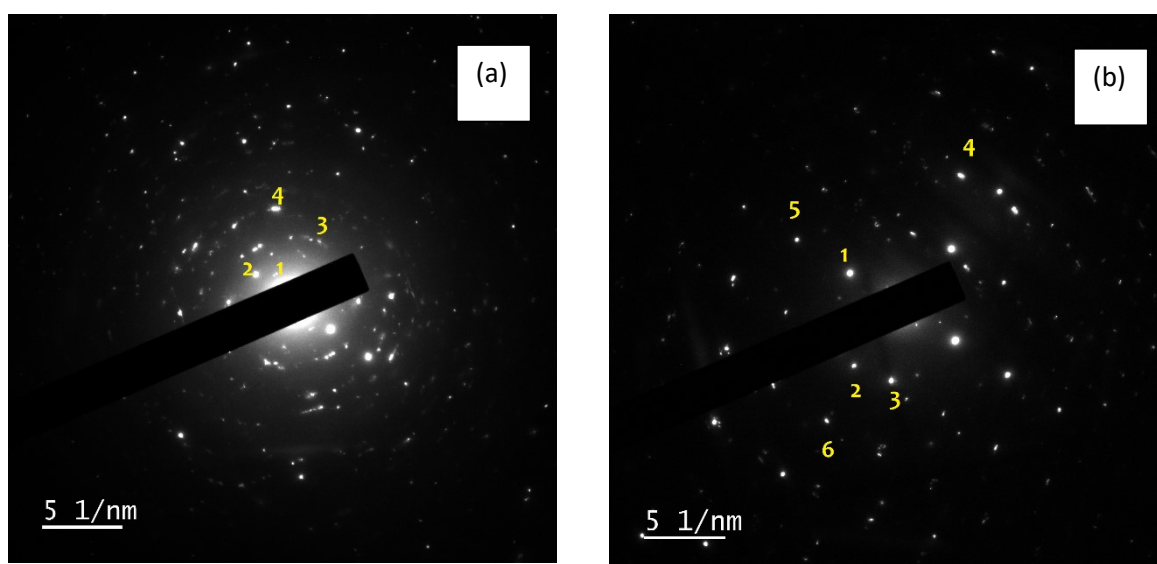


Fig. S5. SAED images of (a) MZN-1 and (b) MZN-2.

Table S6: SAED analysis of MZN-2

	Area	Mean	Min	Max	Angle	Length (1/D)	Length (1/r) (/nm)	r (nm)	d spacing (Å)
1	0.139	43.87	0.403	255	-32.72	7.968	3.984	0.25	2.5
2	0.17	25.756	0.351	255	129.597	9.787	4.893	0.2	2
3	0.162	42.921	0.344	255	114.745	9.306	4.653	0.2149	2.149
4	0.322	25.163	0.331	255	106.189	18.5	9.25	0.108	1.08
5	0.277	45.57	0.385	255	-32.562	15.906	7.953	0.125	1.25
6	0.318	25.159	0.516	255	127.077	18.266	9.133	0.109	1.09



Fig. S6. Zeta potential measurement of (a) MZN-1 and (b) MZN-2.

The Stern-Volmer equation:

$$\frac{F_0}{F} = 1 + K_{SV}[Q] \dots\dots\dots(S1)$$

where, F_0 and F represents fluorescent intensity of the MOF suspension at a particular wavelength in the absence and presence of quencher respectively, K_{SV} (L/mol) is the Stern-Volmer constant and $[Q]$ (nmol/L) is the concentration of the quencher.

The LOD value was calculated using the following formula

$$LOD = \frac{3\sigma}{S} \dots\dots\dots(S2)$$

where, signal/noise = 3, S is the slope of Stern-Volmer linear relationship, σ is the standard deviation.

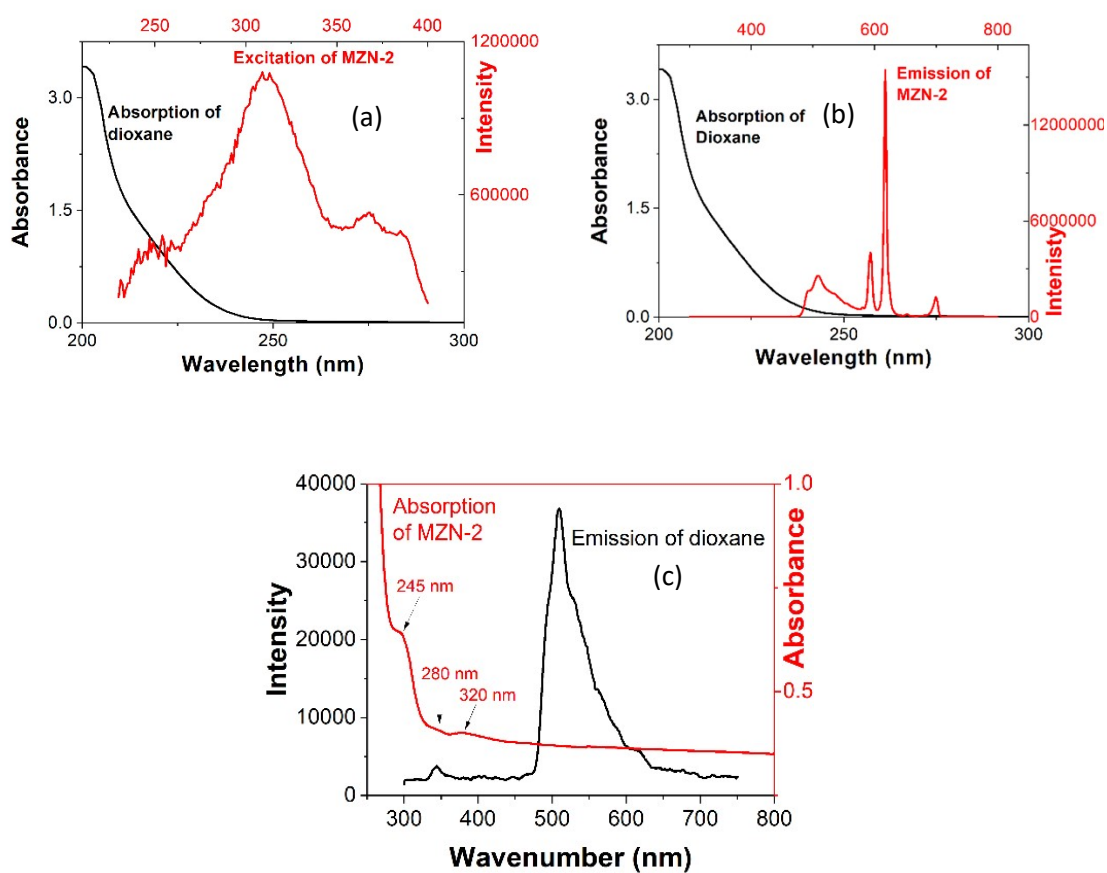


Fig. S7. (a) The comparative plot between absorption spectra of dioxane (absorber) and excitation of MZN-2, (b) The comparative plot between absorption spectra of dioxane (absorber) and emission of MZN-2, (c) FRET study.

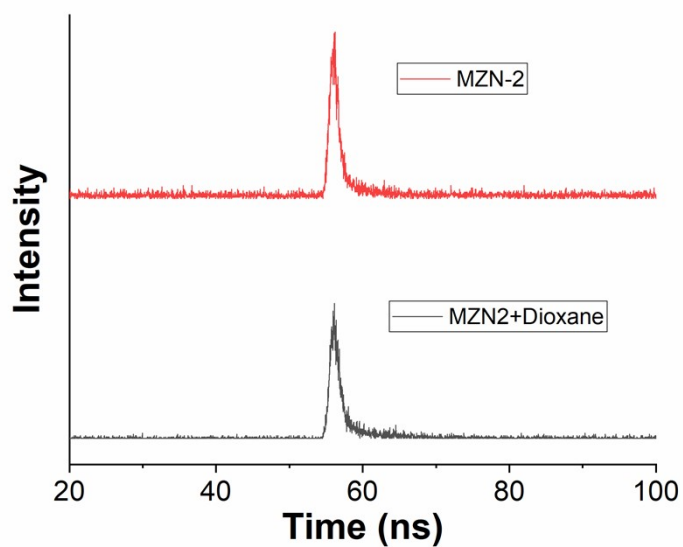


Fig. S8. TRPL plot of MZN2 before and after addition of dioxane, the 617 nm emission peak was considered.

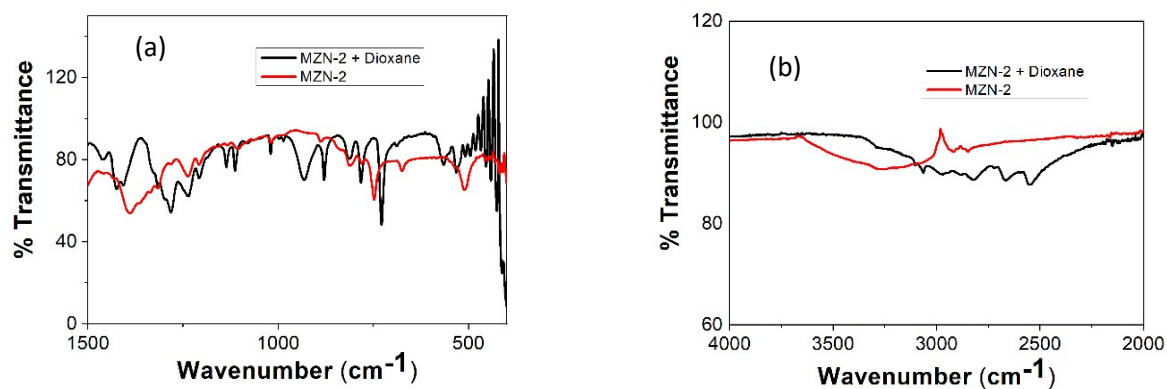


Fig. S9. FTIR spectra of MZN-2 treated with dioxane.

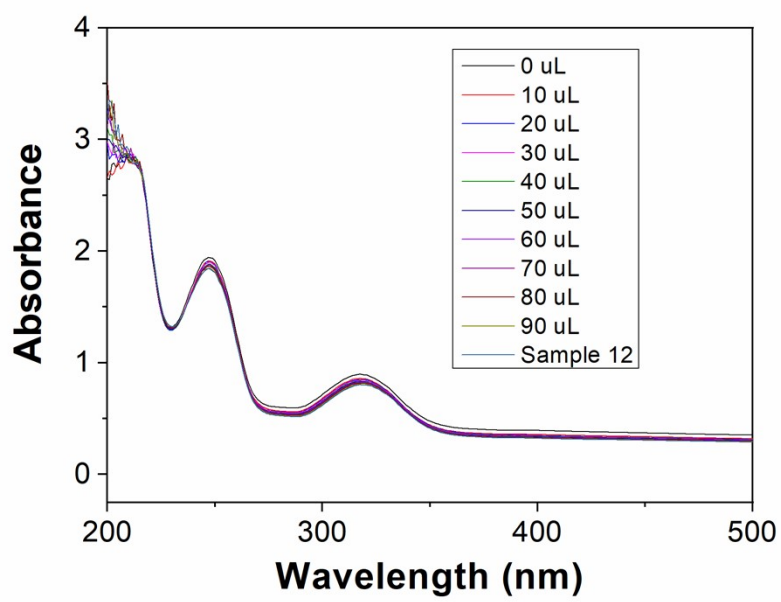


Fig. S10. UV-Visible absorption spectra of MSBCN treated with dioxane

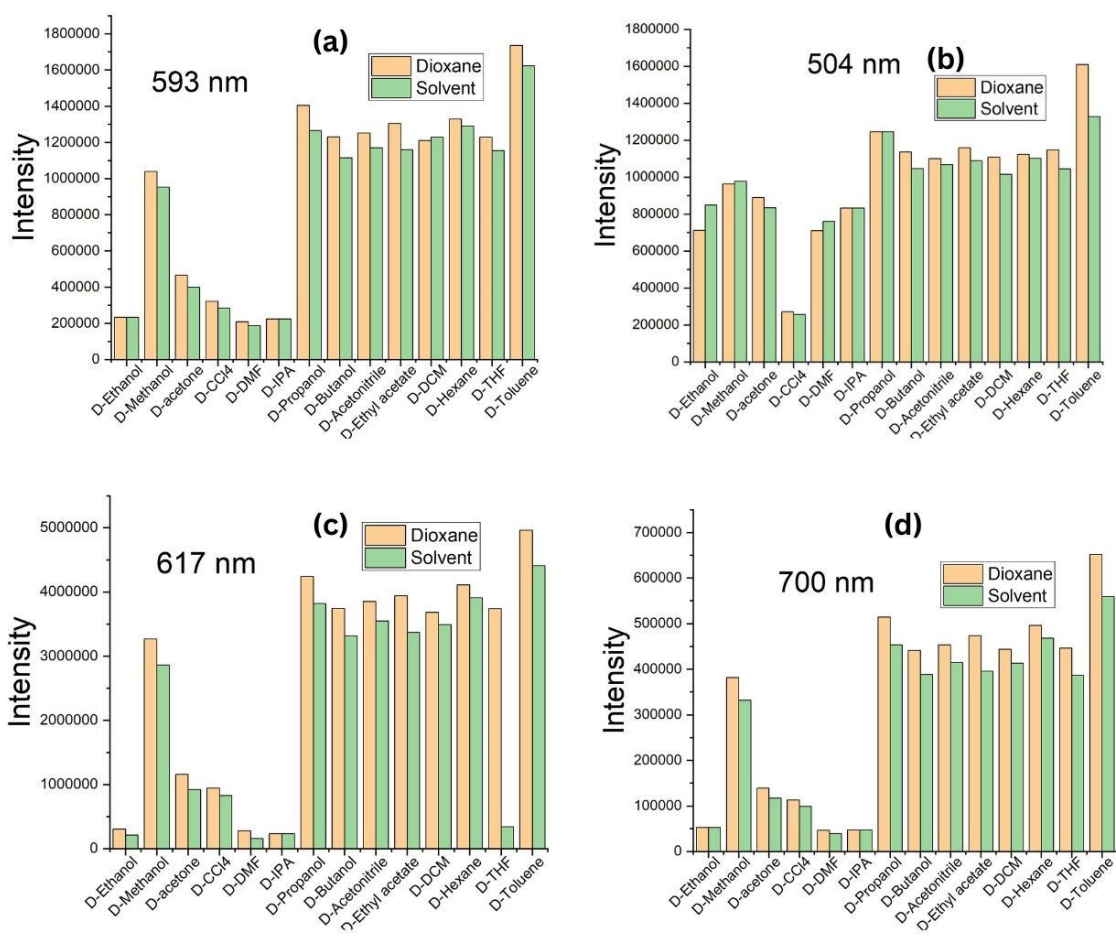


Fig. S11. Selectivity study of MZN-2 towards dioxane in presence of interfering solvents. Emission spectra were recorded by excitement with 270 nm.

Table S7. Comparative table for dioxane sensing

Sl No.	Name of the system	Sensing Experiment	Phase of detection	LOD	Reference
1	PdRu based flavonoid nanocatalyst	Electrochemical	Liquid	0.32 ± 0.0099 ppb	Sustainable Bimetallic Nanocatalysts for Electrochemical Detection and Degradation of 1, 4-Dioxane in Water and Wastewater. Available at SSRN: https://ssrn.com/abstract=4793495
2	AuCu Nanodendrites and MWCNT	Electrochemical	Liquid	3.27 ± 0.04 pM	Electrochemically nanotuned surface comprising 3D bimetallic dendrites fabricated on MWCNT for detection of 1, 4-dioxane in water. <i>Microchemical Journal</i> , 191, 108845, 2023
3	Graphene oxide nanosheet	Electrochemical	Liquid	20.51 nM	Novel statistically optimized one pot synthesis of inherently photoluminescent and electroactive graphene oxide nanosheets as 1, 4 dioxane sensor. <i>Dig J Nanomater Biostructures</i> , 18, 377-388, 2023
4	Curcumin conjugated MWCNT	Electrochemical	Liquid	10 nM	Fabrication of Curcumin-Based Electrochemical Nanosensors for the Detection of Environmental Pollutants: 1, 4-Dioxane and Hydrazine. <i>Biosensors</i> , 14(6), 291, 2024
5	Mixed metal oxide nanoparticle (ZnO/NiO/MnO ₂)	Electrochemical	Liquid	9.14 ± 4.55 pM	Potential application of mixed metal oxide nanoparticle-embedded glassy carbon electrode as a selective 1, 4-dioxane chemical sensor probe by an

					electrochemical approach. RSC advances, 9(72), 42050-42061, 2019
6	Luminescent Porous Organic Polymer	Fluorescence	Liquid	5 ppM	Multifunctional luminescent porous organic polymer for selectively detecting iron ions and 1, 4-dioxane via luminescent turn-off and turn-on sensing. ACS Applied Materials & Interfaces, 8(36), 24097-24103, 2016
7	Amine decorated Cd(II) MOF Parent d10 – MOF functionalized with 1-naphthaldehyde – PSM-1 Benzophenone – PSM-2	Fluorescence	Liquid Gas	PSM-1 = 1.079ppM PSM-2 = 2.487ppM	Amine-substituent induced highly selective and rapid “turn-on” detection of carcinogenic 1, 4-dioxane from purely aqueous and vapour phase with novel post-synthetically modified d 10-MOFs. Dalton Transactions, 51(5), 2083-2093, 2022
8	ZnO/GO nanocomposites	Electrochemical	Liquid	12.34 ± 0.62 pM	Selective 1, 4-dioxane chemical sensor development with doped ZnO/GO nanocomposites by electrochemical approach. Journal of Materials Science: Materials in Electronics, 33(7), 4360-4374, 2022
9	4-amino-1,8-naphthalimide Troger’s base functionalized triazine organic polymer	Fluorescence	Gas	22.2 ppM	“Turn-on” fluorescence sensing of volatile organic compounds using a 4-amino-1, 8-naphthalimide Tröger's base functionalised triazine organic polymer. Chemical communications, 55(81),

					12140-12143, 2019
10	Eu-based MOF from g-C ₃ N ₄ , MoS ₂ and terephthalic acid	Fluorescence	liquid	0.026 ppm	Present technology

Reference:

(S1) Frisch, M. J.; Trucks, G. W.; Schlegel, H. B.; Scuseria, G. E.; Robb, M. A.; Cheeseman, J. R.; Scalmani, G.; Barone, V.; Mennucci, B.; Petersson, G. A.; et al. Gaussian 09, revision D.01; Gaussian, Inc.: Wallingford, CT, 2009.

(S2) Lee, C.; Yang, W.; Parr, R. G. Development of the ColleSalvetti Correlation-energy Formula into a Functional of the Electron Density. *Phys. Rev. B: Condens. Matter Mater. Phys.* 1988, 37, 785-789.

(S3) Zhang, X. I. Synthesis and Crystal Structure of a Complex of Melamine with Benzoic Acid. *Chem Res Chin Univ* 2008, 24 (4), 396–400.

(S4) Ba, T. Le; Alkurdi, A. Q.; Lukács, I. E.; Molnár, J.; Wongwises, S.; Gróf, G.; Szilágyi, I. M. A Novel Experimental Study on the Rheological Properties and Thermal Conductivity of Halloysite Nanofluids. *Nanomaterials* 2020, Vol. 10, Page 1834 2020, 10 (9), 1834.

(S5) Zhou, G.; Wu, M. F.; Xing, Q. J.; Li, F.; Liu, H.; Luo, X. B.; Zou, J. P.; Luo, J. M.; Zhang, A. Q. Synthesis and Characterizations of Metal-Free Semiconductor/MOFs with Good Stability and High Photocatalytic Activity for H₂ Evolution: A Novel Z-Scheme Heterostructured Photocatalyst Formed by Covalent Bonds. *Appl Catal B* 2018, 220, 607–614.